Title: Metabolite therapy guided by liquid biopsy proteomics delays retinal neurodegeneration

Authors: Katherine J. Wert[1,*], Gabriel Velez[1,2,*], Vijaya L. Kanchustambham[3], Vishnu Shankar[3], Lucy P. Evans[4], Jesse D. Sengillo[5], Richard N. Zare[3], Alexander G. Bassuk[4], Stephen H. Tsang[6,7,8], Vinit B. Mahajan[1,9]

Affiliations:

[1]Omics Laboratory, Byers Eye Institute, Department of Ophthalmology, Stanford University, Palo Alto, CA 94304

[2]Medical Scientist Training Program, Carver College of Medicine, University of Iowa, Iowa City, IA 52242

[3]Department of Chemistry, Stanford University, Stanford, CA 94305

[4]Departments of Pediatrics and Neurology, Carver College of Medicine, University of Iowa, Iowa City, IA 52242

[5]Bascom Palmer Eye Institute, University of Miami Miller School of Medicine, Miami, FL 33136

[6]Edward S. Harkness Eye Institute, New York-Presbyterian Hospital, New York, NY 10032

[7]Jonas Children's Vision Care and Bernard & Shirlee Brown Glaucoma Laboratory, Department of Ophthalmology, Vagelos College of Physicians and Surgeons, Columbia University, New York, NY 10032

[8]Department of Pathology & Cell Biology, Stem Cell Initiative (CSCI), Institute of Human Nutrition, Vagelos College of Physicians and Surgeons, Columbia University, New York, NY 10032

[9]Veterans Affairs Palo Alto Health Care System, Palo Alto, CA 94304

*Co-first authors

Corresponding Author: Vinit B. Mahajan, Byers Eye Institute, Department of Ophthalmology, Stanford University, Palo Alto, CA, 94304 USA. Phone: 650-723-6995. Fax: 650-498-1528. E-mail: vinit.mahajan@stanford.edu

List of Supplementary Materials:

Supplementary Figures

Fig. S1. Gene ontology of the *Pde6a*^{D670G} retina at different stages of degeneration.

Fig. S2. Gene ontology of the *Pde6a*^{D670G} vitreous at different stages of degeneration.

Fig. S3. Gene ontology distributions of candidate vitreous biomarkers.

Fig. S4. DESI-MSI chemical maps of retina from wild-type, arRP, and α-KG treated mice.

Fig. S5. DESI-MSI chemical maps of whole eye from wild-type, arRP, and α-KG treated mice.

Fig. S6. Tandem-MS analysis of extracted metabolites from the retinal tissue.

Fig. S7. DESI-MS analysis of extracted metabolites from the retinal tissue.

Fig. S8. Distribution of α-KG across wild-type, arRP, and α-KG treated mice.

Supplementary Tables

Table S1. Vitreous biopsies from arRP patients and unaffected controls.

Table S2. Proteomic content of human vitreous samples by LC-MS/MS analysis.

Table S3. Relative quantification of proteins identified in human vitreous samples.

Table S4. Proteomic content of *Pde6a*^{D670G} retina and vitreous by LC-MS/MS analysis.

Table S5. Distinct peptides identified in *Pde6a*^{D670G} retina and vitreous samples.

Table S6. Protein groups identified in *Pde6a*^{D670G} retina and vitreous samples.

Table S7. Relative quantification and comparison of proteins identified in *Pde6a*^{D670G} retina samples.

Table S8. Relative quantification and comparison of proteins identified in *Pde6a*^{D670G} vitreous samples.

Table S9. Differentially-expressed *Pde6a*^{D670G} retina and vitreous proteins in all disease stages.

Table S10. Differentially-expressed *Pde6a*^{D670G} retina and vitreous proteins in early disease stages.

Table S11. Candidate biomarkers from *Pde6a*^{D670G} vitreous samples.

Table S12. Pathway representation of down-regulated proteins in the *Pde6a*^{D670G} retina.

Table S13. Down-regulated proteins in the *Pde6a*^{D670G} retina involved in oxidative phosphorylation.

Table S14. Down-regulated proteins in the *Pde6a*^{D670G} retina involved in the tricarboxylic acid (TCA) cycle.

Table S15. Down-regulated proteins in the *Pde6a*^{D670G} retina involved in rod outer segment phototransduction.

Table S16. Tandem-MS analysis of extracted metabolites from the retinal tissue.

Supplementary Figures

Fig. S1

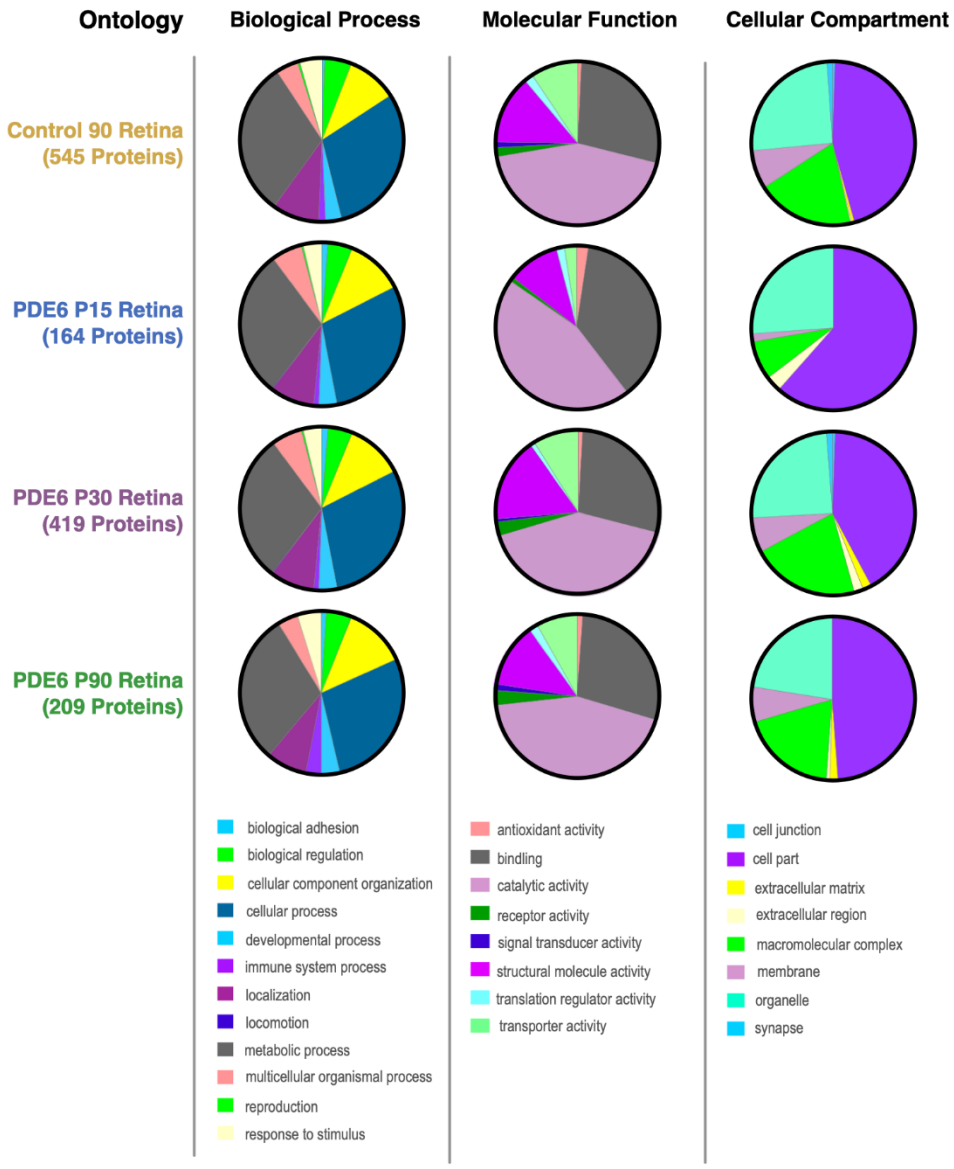

Fig. S2


Ontology
Biological Process
Molecular Function
Cellular Compartment
Control 90 Vitreous (100 Proteins)
PDE6 P15 Vitreous (568 Proteins)
PDE6 P30 Vitreous (40 Proteins)
PDE6 P90 Vitreous (226 Proteins)
biological adhesion
biological regulation
cellular component organization
cellular process
developmental process
immune system process
localization
locomotion
metabolic process
multicellular organismal process
reproduction
response to stimulus
antioxidant activity
bindling
catalytic activity
receptor activity
signal transducer activity
structural molecule activity
translation regulator activity
transporter activity
cell junction
cell part
extracellular matrix
extracellular region
macromolecular complex
membrane
organelle
synapse

Fig. S3

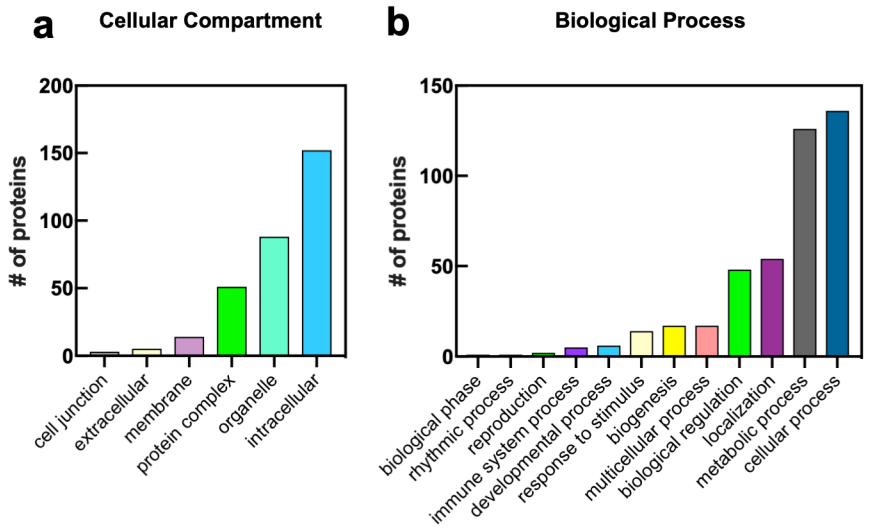
a
Cellular Compartment
# of proteins
200
150
100
50
0
cell junction
extracellular
membrane
protein complex
organelle
intracellular
b
Biological Process
# of proteins
150
100
50
0
biological phase
rhythmic process
reproduction
immune system process
developmental process
response to stimulus
biogenesis
multicellular process
biological regulation
localization
metabolic process
cellular process

Fig. S4

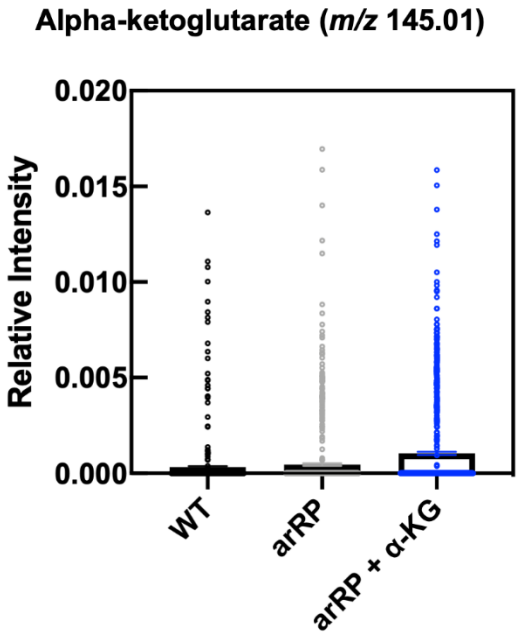
Alpha-ketoglutarate (*m/z* 145.01)
Relative Intensity
0.020
0.015
0.010
0.005
0.000
WT
arRP
arRP + α-KG

Fig. S5

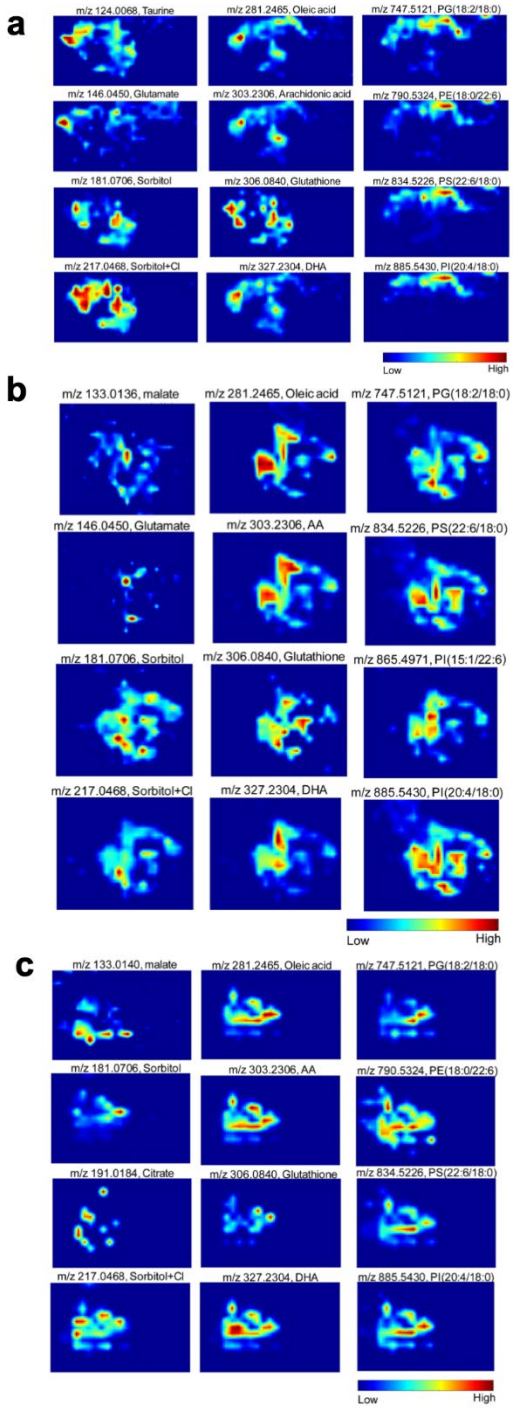
a
m/z 124.0068, Taurine
m/z 281.2465, Oleic acid
m/z 747.5121, PG(18:2/18:0)
m/z 146.0450, Glutamate
m/z 303.2306, Arachidonic acid
m/z 790.5324, PE(18:0/22:6)
m/z 181.0706, Sorbitol
m/z 306.0840, Glutathione
m/z 834.5226, PS(22:6/18:0)
m/z 217.0468, Sorbitol+Cl
m/z 327.2304, DHA
m/z 885.5430, PI(20:4/18:0)
Low
High
b
m/z 133.0136, malate
m/z 281.2465, Oleic acid
m/z 747.5121, PG(18:2/18:0)
m/z 146.0450, Glutamate
m/z 303.2306, AA
m/z 834.5226, PS(22:6/18:0)
m/z 181.0706, Sorbitol
m/z 306.0840, Glutathione
m/z 865.4971, PI(15:1/22:6)
m/z 217.0468, Sorbitol+Cl
m/z 327.2304, DHA
m/z 885.5430, PI(20:4/18:0)
Low
High
c
m/z 133.0140, malate
m/z 281.2465, Oleic acid
m/z 747.5121, PG(18:2/18:0)
m/z 181.0706, Sorbitol
m/z 303.2306, AA
m/z 790.5324, PE(18:0/22:6)
m/z 191.0184, Citrate
m/z 306.0840, Glutathione
m/z 834.5226, PS(22:6/18:0)
m/z 217.0468, Sorbitol+Cl
m/z 327.2304, DHA
m/z 885.5430, PI(20:4/18:0)
Low
High

Fig. S6

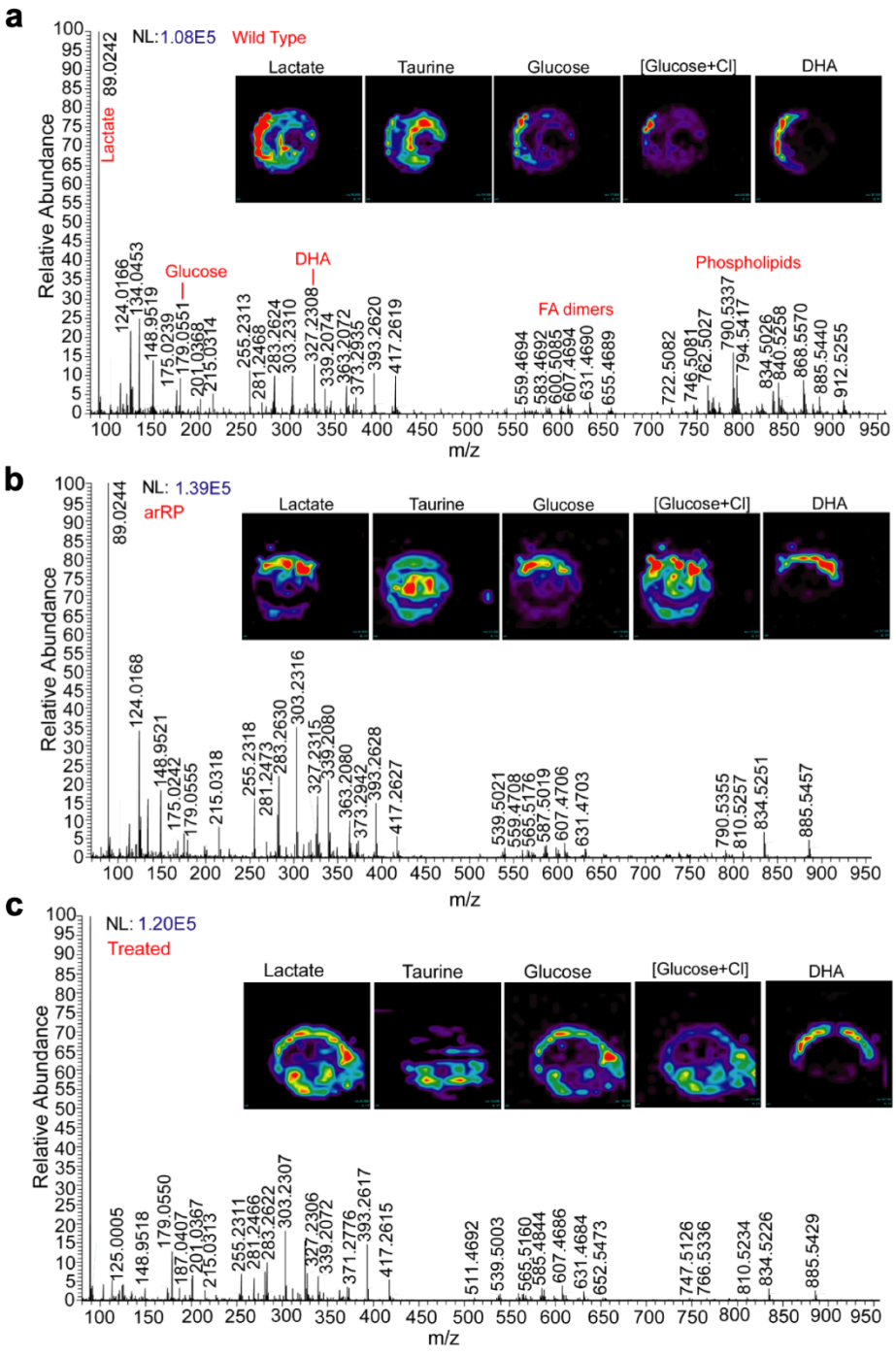
a
NL:1.08E5 Wild Type
Lactate
Taurine
Glucose
[Glucose+Cl]
DHA
Relative Abundance
m/z
Lactate
Glucose
DHA
FA dimers
Phospholipids
b
NL: 1.39E5
arRP
c
NL: 1.20E5
Treated

Fig. S7

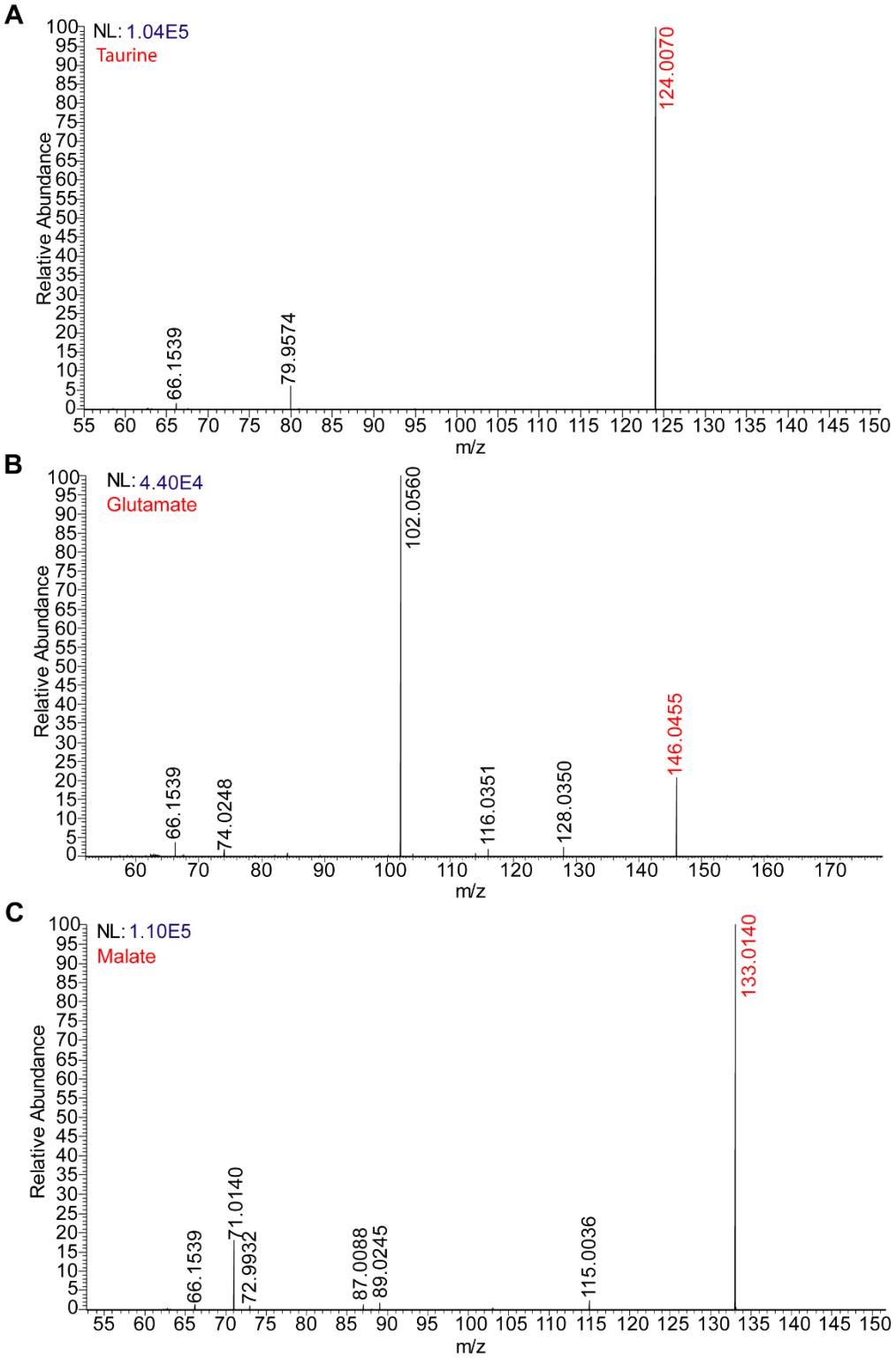
A
NL: 1.04E5
Taurine
124.0070
66.1539
79.9574
Relative Abundance
m/z
B
NL: 4.40E4
Glutamate
102.0560
146.0455
66.1539
74.0248
116.0351
128.0350
Relative Abundance
m/z
C
NL: 1.10E5
Malate
133.0140
71.0140
66.1539
72.9932
87.0088
89.0245
115.0036
Relative Abundance
m/z

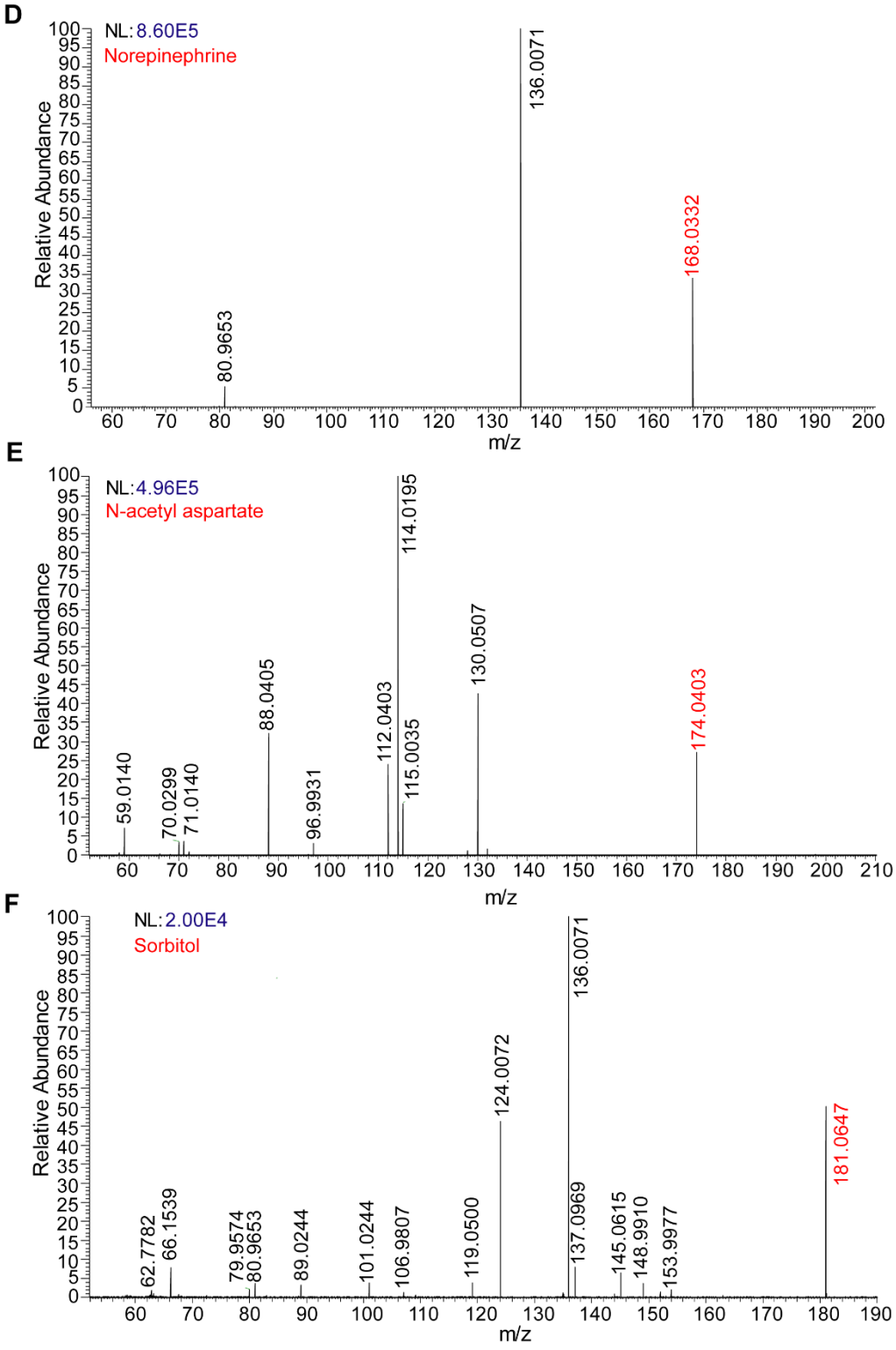
D
NL:8.60E5
Norepinephrine
Relative Abundance
m/z
80.9653
136.0071
168.0332
E
NL:4.96E5
N-acetyl aspartate
Relative Abundance
m/z
59.0140
70.0299
71.0140
88.0405
96.9931
112.0403
114.0195
115.0035
130.0507
174.0403
F
NL:2.00E4
Sorbitol
Relative Abundance
m/z
62.7782
66.1539
79.9574
80.9653
89.0244
101.0244
106.9807
119.0500
124.0072
136.0071
137.0969
145.0615
148.9910
153.9977
181.0647

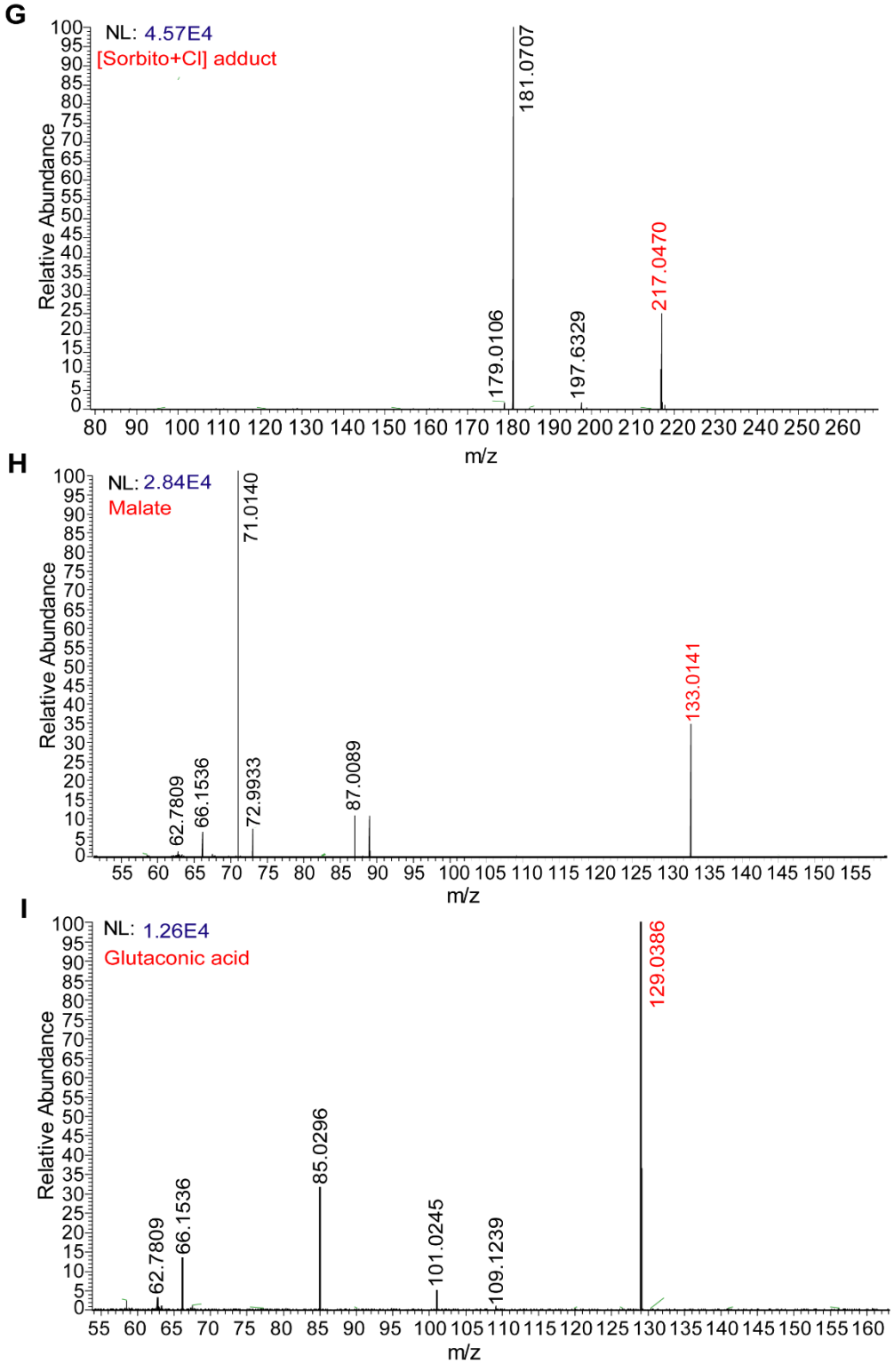
G
NL: 4.57E4
[Sorbito+Cl] adduct
Relative Abundance
m/z
181.0707
217.0470
179.0106
197.6329
H
NL: 2.84E4
Malate
71.0140
133.0141
62.7809
66.1536
72.9933
87.0089
I
NL: 1.26E4
Glutaconic acid
129.0386
85.0296
62.7809
66.1536
101.0245
109.1239

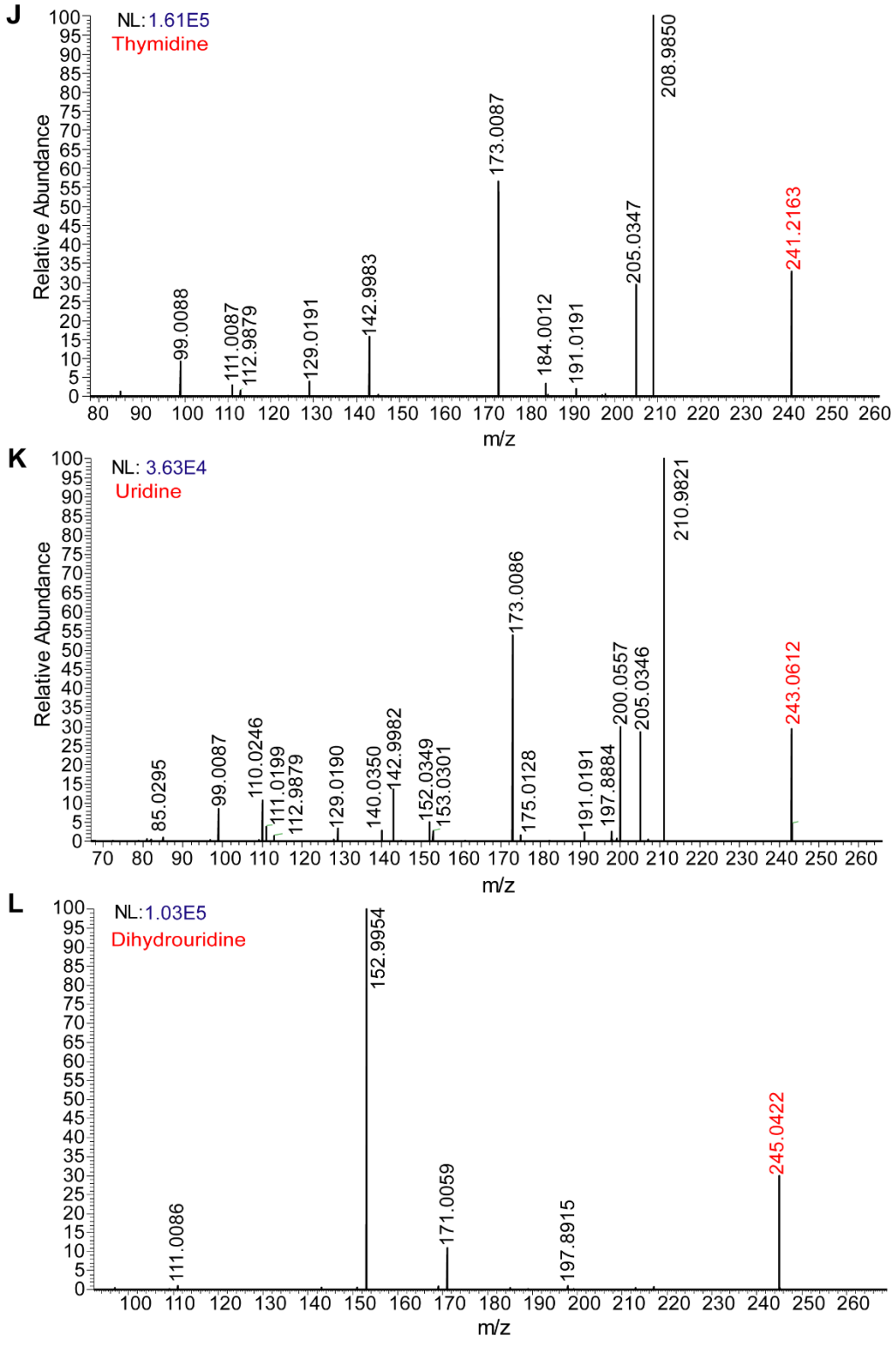
J
NL: 1.61E5
Thymidine
Relative Abundance
m/z
99.0088
111.0087
112.9879
129.0191
142.9983
173.0087
184.0012
191.0191
205.0347
208.9850
241.2163
K
NL: 3.63E4
Uridine
85.0295
99.0087
110.0246
111.0199
112.9879
129.0190
140.0350
142.9982
152.0349
153.0301
173.0086
175.0128
191.0191
197.8884
200.0557
205.0346
210.9821
243.0612
L
NL: 1.03E5
Dihydrouridine
111.0086
152.9954
171.0059
197.8915
245.0422

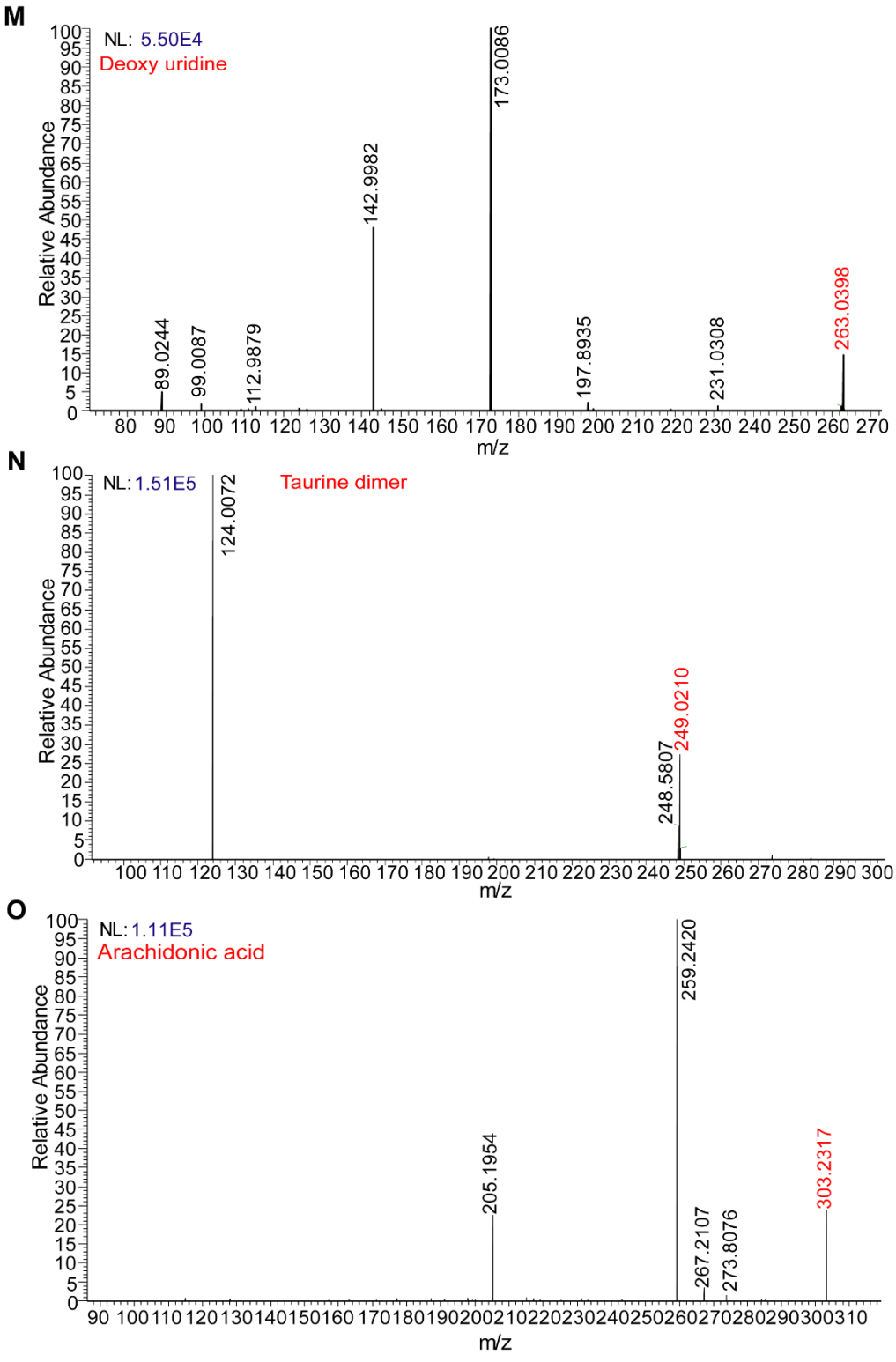
M
NL: 5.50E4
Deoxy uridine
Relative Abundance
m/z
89.0244
99.0087
112.9879
142.9982
173.0086
197.8935
231.0308
263.0398
N
NL: 1.51E5
Taurine dimer
124.0072
248.5807
249.0210
O
NL: 1.11E5
Arachidonic acid
205.1954
259.2420
267.2107
273.8076
303.2317

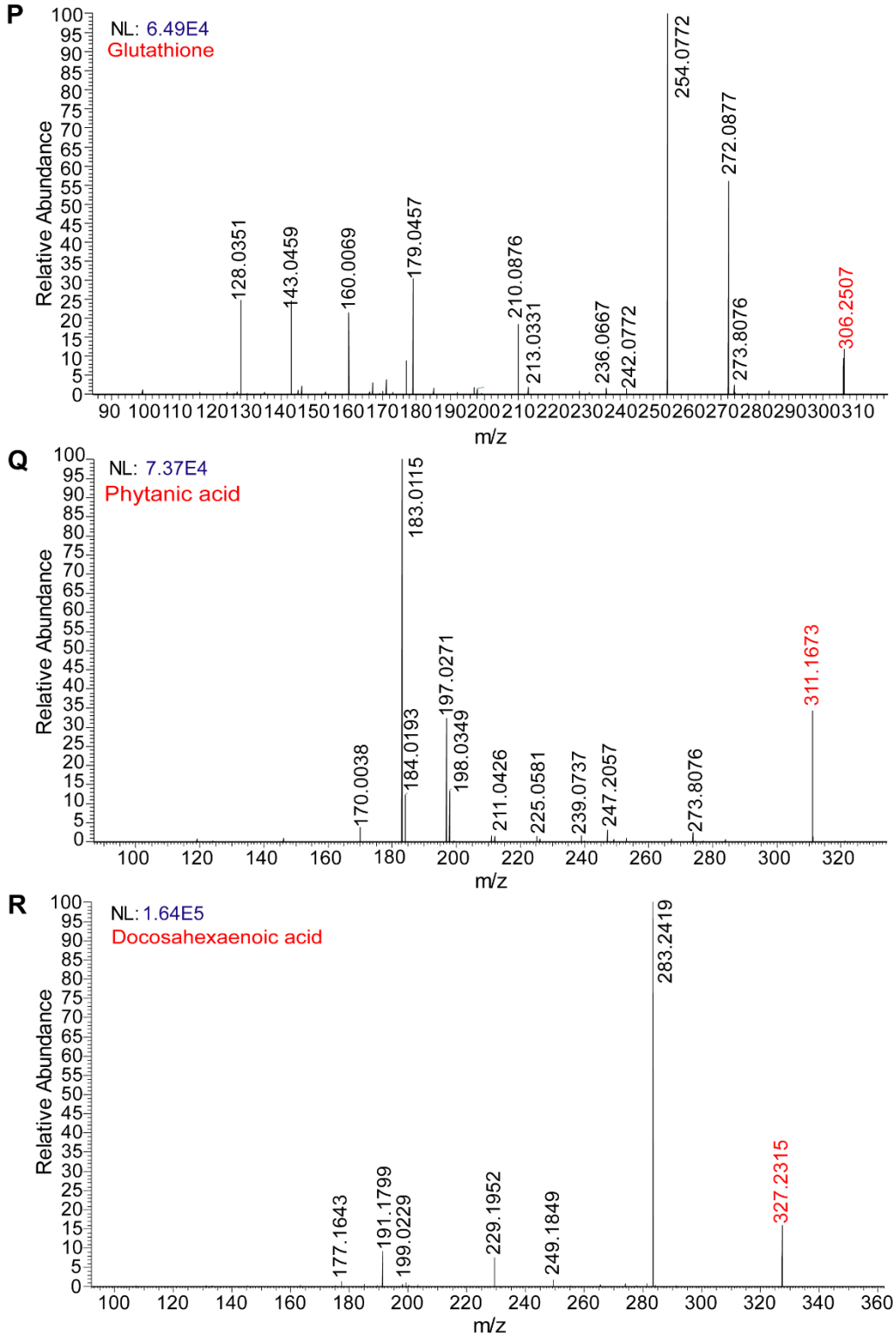
P
NL: 6.49E4
Glutathione
Relative Abundance
m/z
128.0351
143.0459
160.0069
179.0457
210.0876
213.0331
236.0667
242.0772
254.0772
272.0877
273.8076
306.2507
Q
NL: 7.37E4
Phytanic acid
Relative Abundance
m/z
170.0038
183.0115
184.0193
197.0271
198.0349
211.0426
225.0581
239.0737
247.2057
273.8076
311.1673
R
NL: 1.64E5
Docosahexaenoic acid
Relative Abundance
m/z
177.1643
191.1799
199.0229
229.1952
249.1849
283.2419
327.2315

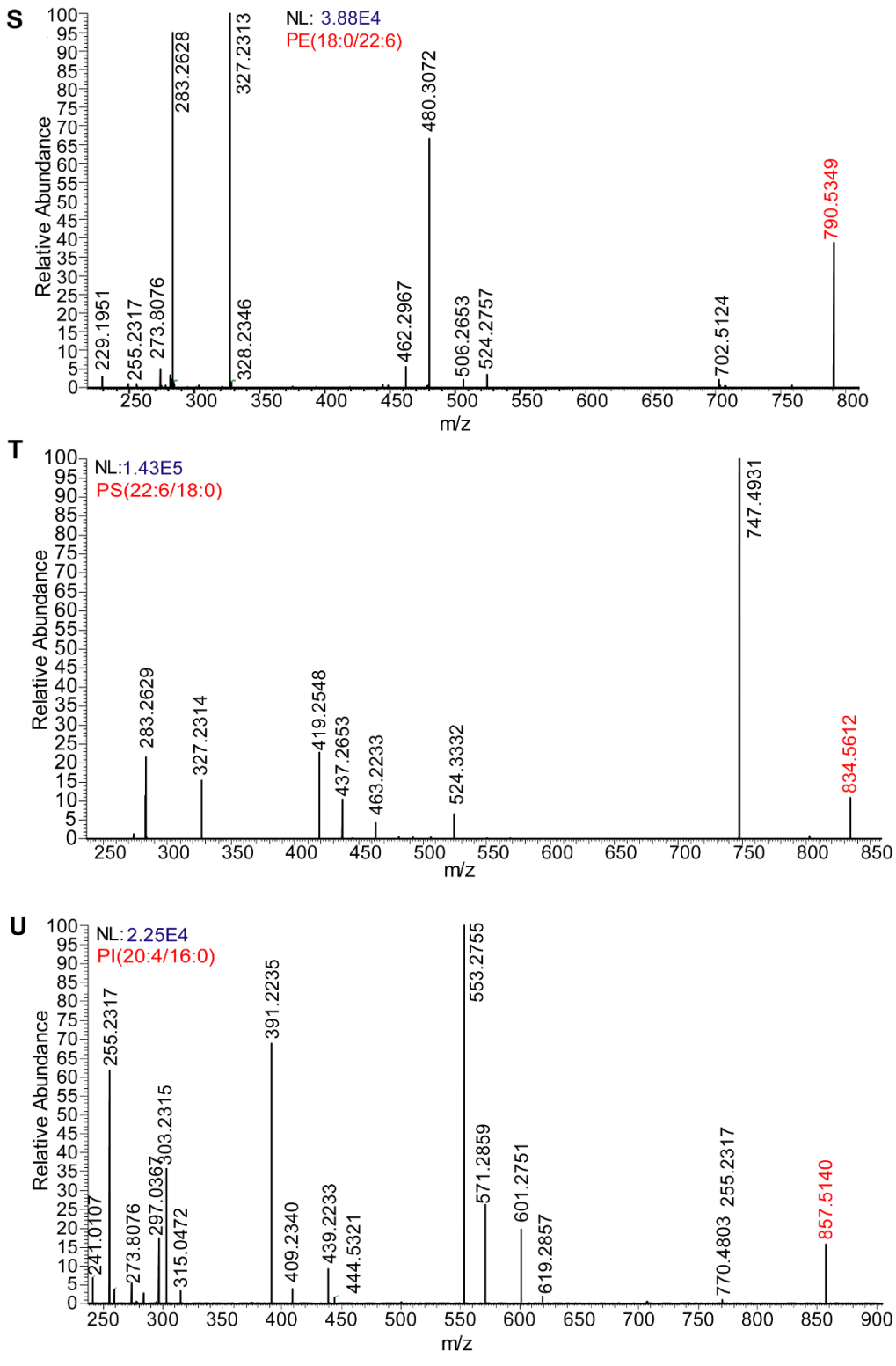
S
NL: 3.88E4
PE(18:0/22:6)
Relative Abundance
m/z
229.1951
255.2317
273.8076
283.2628
327.2313
328.2346
462.2967
480.3072
506.2653
524.2757
702.5124
790.5349
T
NL:1.43E5
PS(22:6/18:0)
Relative Abundance
m/z
283.2629
327.2314
419.2548
437.2653
463.2233
524.3332
747.4931
834.5612
U
NL:2.25E4
PI(20:4/16:0)
Relative Abundance
m/z
241.0107
255.2317
273.8076
297.0367
303.2315
315.0472
391.2235
409.2340
439.2233
444.5321
553.2755
571.2859
601.2751
619.2857
770.4803
255.2317
857.5140

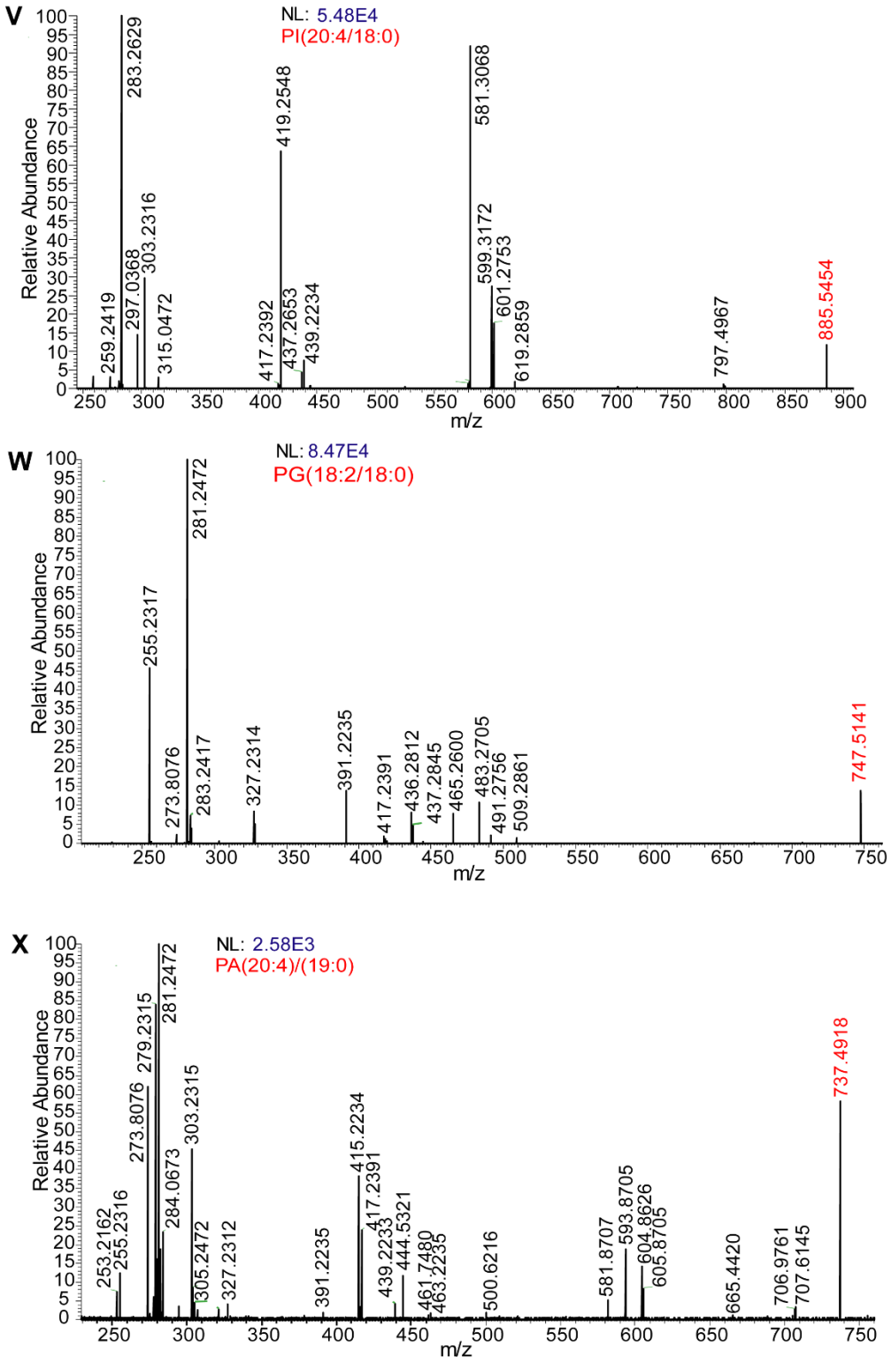
V
NL: 5.48E4
PI(20:4/18:0)
Relative Abundance
m/z
283.2629
419.2548
581.3068
303.2316
297.0368
599.3172
601.2753
315.0472
259.2419
417.2392
437.2653
439.2234
619.2859
797.4967
885.5454
W
NL: 8.47E4
PG(18:2/18:0)
281.2472
255.2317
273.8076
283.2417
327.2314
391.2235
417.2391
436.2812
437.2845
465.2600
483.2705
491.2756
509.2861
747.5141
X
NL: 2.58E3
PA(20:4)/(19:0)
281.2472
279.2315
273.8076
303.2315
284.0673
415.2234
417.2391
253.2162
255.2316
305.2472
327.2312
391.2235
439.2233
444.5321
461.7480
463.2235
500.6216
581.8707
593.8705
604.8626
605.8705
665.4420
706.9761
707.6145
737.4918

Fig. S8

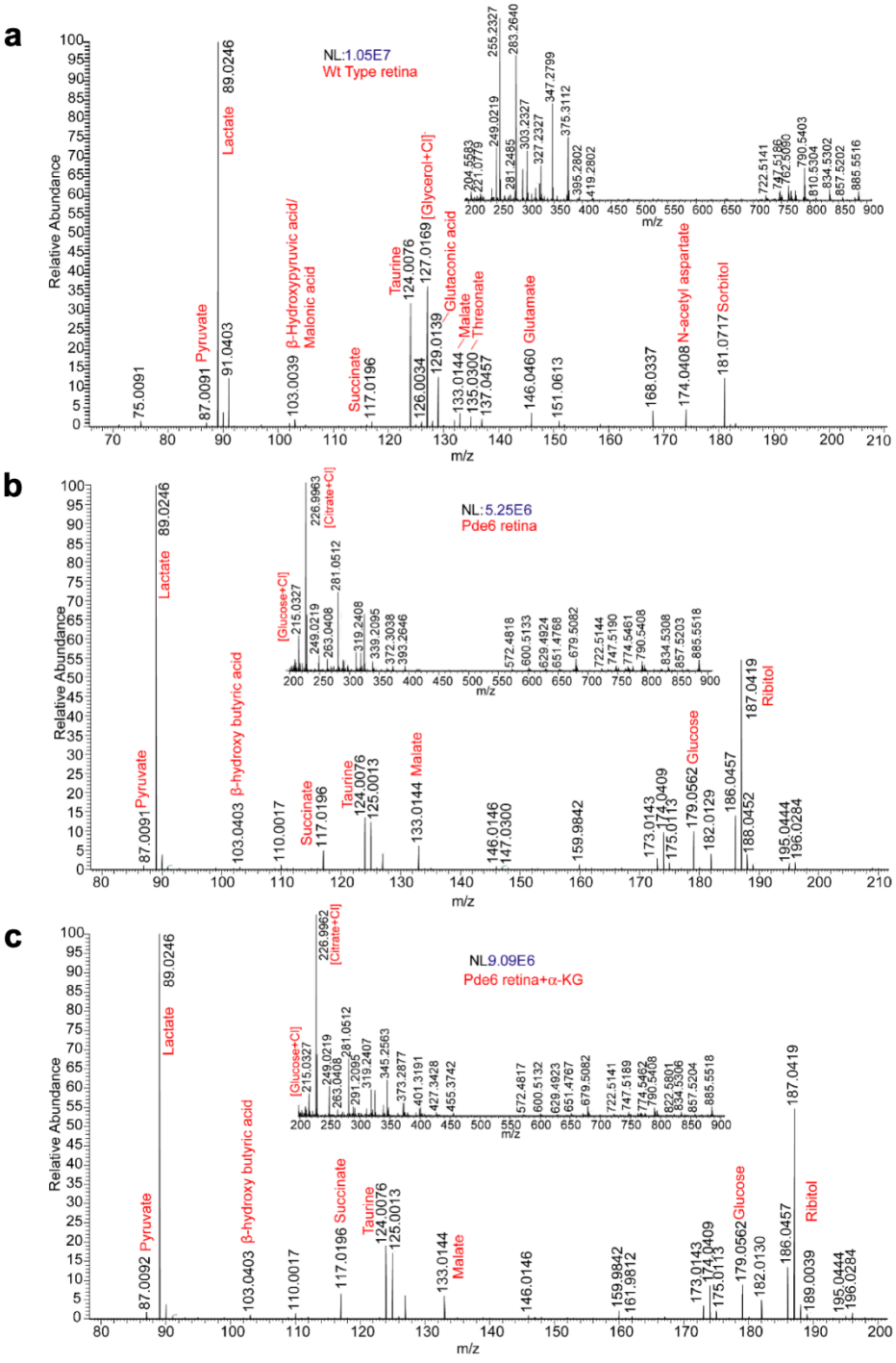
a
NL:1.05E7
Wt Type retina
Lactate
Pyruvate
β-Hydroxypyruvic acid/
Malonic acid
Succinate
Taurine
Glutaconic acid
Malate
Threonate
Glutamate
N-acetyl aspartate
Sorbitol
[Glycerol+Cl]
b
NL:5.25E6
Pde6 retina
β-hydroxy butyric acid
[Glucose+Cl]
[Citrate+Cl]
Glucose
Ribitol
c
NL9.09E6
Pde6 retina+α-KG
Relative Abundance
m/z

Supplementary Figure Legends

Fig. S1. Gene ontology (GO) distributions of retina samples. Identified retinal proteins from the wild-type and *Pde6a*^{D670G} mice at P15, P28, and P90. Gene ontology analysis categorized each protein group by biological process, molecular function, and cellular compartment.

Fig. S2. Gene ontology (GO) distributions of vitreous samples. Identified vitreous proteins from the wild-type and *Pde6a*^{D670G} mice at P15, P28, and P90. Gene ontology analysis categorized each protein group by biological process, molecular function, and cellular compartment.

Fig. S3. Gene ontology (GO) distributions of candidate vitreous biomarkers. Gene ontology (GO) categorization of the 446 protein biomarkers by **(a)** cellular compartment and **(b)** biological process.

Fig. S4. DESI-MSI chemical maps of retina. The 2D-chemical maps of individual metabolites are shown for **(a)** wild-type **(b)** arRP and **(c)** α-KG treated mice. PA, phosphatidic acid; PE, phosphatidylethanolamine; PG, phosphatidylglycerol; PI, phosphatidylinositol; PS, phosphatidylserine; DHA, docosahexaenoic acid, CI, collision induced.

Fig. S5. DESI-MSI chemical maps of whole eye. The respective raw MS spectrum across all the pixels in a row and the 2D-chemical maps of individual metabolites is shown for **(a)** wild-type **(b)** arRP and **(c)** α-KG treated mice. NL, normalization level.

Fig. S6. Tandem-MS analysis of extracted metabolites from the retinal tissue: Collision induced dissociation analysis (CID), is shown for small metabolites, fatty acids, and lipids to identify molecular species based on fragmentation pattern: **(a)** Taurine; **(b)** Glutamate; **(c)** Malate; **(d)** Norepinephrine; **(e)** N-acetyl aspartate; **(f)** Sorbitol; **(g)** [Sorbitol + collision-induced (CI)] adduct; **(h)** Malate; **(i)** Glutaconic acid; **(j)** Thymidine; **(k)** Uridine; **(l)** Dihydro-uridine; **(m)** Deoxy-uridine; **(n)** Taurine (dimer); **(o)** Arachidonic acid; **(p)** Glutathione; **(q)** Phytanic acid. **(r)** Docosahexaenoic acid (DHA); **(s)** Phosphatidylethanolamine (PE, 18:0/22:6). **(t)** Phosphatidylserine (PS, 22:6/18:0). **(u)** Phosphatidylinositol (PI, 20:4/16:0). **(v)** Phosphatidylinositol (PI, 20:4/18:0). **(w)** Phosphatidylglycerol (PG, 18:2/18:0). **(x)** Phosphatidic acid (PA, 20:4/19:0). **(y)** 5-LGlutamyl-L-alanine. **(z)** Phosphatidylserine (PS, 18:0/20:4). NL, normalization level.

Fig. S7. DESI-MS analysis of extracted metabolites from the retinal tissue: Electrospray ionization is performed on the retina tissue extraction in solvents in the mass range *m/z* 50-1000. Red labels denote peaks assigned to identified metabolites and lipids. NL, normalization level. Results are displayed as the relative intensity of the corresponding metabolite normalized by the total ion current (sum of all intensity values from the detected ions).

Fig. S8. Distribution of α-KG across wild-type, arRP, and α-KG treated mice: Levels of α-KG (*m/z* 145.01) are not significantly different between arRP and treated mice (fold change 1.26, false discovery rate < 0.05). The supplemental α-KG in treated state is consumed and reflected in the increased intensity of other metabolites in TCA and glutamate-glutamine conversion pathways.